

# Less Memory Means smaller GPUs: Backpropagation with Compressed Activations

Daniel Barley<sup>1</sup>[0009–0006–1607–1876] and Holger Fröning<sup>1</sup>[0000–0001–9562–0680]

Computing Systems Group, ZITI, Heidelberg University, Heidelberg, Germany  
{daniel.barley,holger.froening}@ziti.uni-heidelberg.de

**Abstract.** The ever-growing scale of deep neural networks (DNNs) has lead to an equally rapid growth in computational resource requirements. Many recent architectures, most prominently Large Language Models, have to be trained using supercomputers with thousands of accelerators, such as GPUs or TPUs. Next to the vast number of floating point operations the memory footprint of DNNs is also exploding. In contrast, GPU architectures are notoriously short on memory. Even comparatively small architectures like some *EfficientNet* variants cannot be trained on a single consumer-grade GPU at reasonable mini-batch sizes. During training, intermediate input activations have to be stored until backpropagation for gradient calculation. These make up the vast majority of the memory footprint. In this work we therefore consider compressing activation maps for the backward pass using pooling, which can reduce both the memory footprint and amount of data movement. The forward computation remains uncompressed. We empirically show convergence and study effects on feature detection at the example of the common vision architecture *ResNet*. With this approach we are able to reduce the peak memory consumption by 29% at the cost of a longer training schedule, while maintaining prediction accuracy compared to an uncompressed baseline.

**Keywords:** Compression, Deep Neural Networks, Training, Backpropagation

## 1 Introduction

The exponential growth of DNNs over the recent years in both parameter count and computational complexity has sparked many advances in GPU technology and vice versa. GPUs meanwhile feature special matrix multiply and most recently even transformer accelerators<sup>1</sup>. These advancements of course allow for even larger DNNs, forming a feedback loop. One of the major bottlenecks in this race is memory. GPU architectures are notoriously short on memory, which is in direct conflict with the ever-growing parameter counts. Different forms of

<sup>1</sup> NVIDIA H100 transformer engine <https://developer.nvidia.com/blog/nvidia-hopper-architecture-in-depth/>

pruning, quantization, and compression of DNNs have therefore become active fields of research.

Pruning aims to lower the memory complexity by moving parts of a network toward zero, which can then be encoded using a sparse format or dropped entirely. For weights, a loss penalty term can be used to encourage more zero values for example. The granularity of pruning can range from individual weights [10] to channels [5] to whole layers of a network [14]. Pruning is of course not limited to weights, but can also be applied to gradients [16] or activations [1].

Quantization on the other hand aims to reduce the memory footprint and computational cost by reducing the bit width of parameters. This includes for example half-precision floating point representations [9] and even integer types [18,7]. In the most extreme cases networks are binarized [11], replacing the more complex integer or floating point arithmetic with bitwise operations.

Pruning and quantization are not mutually exclusive of course. As both can have serious implications on model accuracy and performance [13], finding configurations that maintain accuracy while improving performance is a non-trivial task. Automated approaches can help to navigate the vast search space [8].

A commonality among most of these approaches is them focusing on model inference. Because model inference is often performed on devices orders of magnitude less powerful than the hardware used for training said model this is a necessity of course. This even extends to architectural design. Architectures like *MobileNet* [6] and *EfficientNet* [15] make heavy use of weight sharing and separable convolutions. While only a few hundred megabytes in size during forward inference, training these models produces several gigabytes of intermediate activations needed for backpropagation, more than is available on most consumer-grade or embedded devices. In fact, as shown later in this work, activations are responsible for the vast majority of the memory footprint across architectures during training. The previous example might only be a problem for hobbyists, but scaling to larger architectures, like language models in particular, the memory demands affect even research facilities. Additionally, lowering the memory requirements may enable online learning or fine tuning on smaller devices like the NVIDIA Jetson platforms for example<sup>2</sup>.

To address this issue, we propose a method to compress stored activations during the training process. We use pooling to reduce the dimensions of stored activations and thereby also their memory footprint. In theory this can also reduce the number of memory transactions during gradient computation in the backward pass. To take full advantage, a custom operator is needed however, which is still in development. The forward pass remains unchanged. We only apply the pooling immediately before storing the activation for backpropagation. This ensures an accurate loss computation. Also, unlike sparse approaches, a pooled activation does not require any additional encoding that causes overhead except for the original shape.

---

<sup>2</sup> <https://developer.nvidia.com/embedded-computing>

We test the effects of compressed activations on convergence and memory on *ResNet* [4]. Additionally, we analyze the gradient alignment between a regularly trained model and a compressed one to obtain layer-wise sensitivity information.

In summary, this work makes the following contributions:

1. We characterize various neural architectures regarding their memory footprint, demonstrating the amount of memory consumed by activations.
2. We propose a method to reduce activation space by pooling blocks of activations based on averaging blocks of activations.
3. We assess the implications of the proposed methods for different block sizes on ResNet. Experiments include observed loss curves for different compression configurations, reporting achieved memory size reduction, as well as trading among less memory size and an increased number of epochs to maintain test accuracy.

## 2 Related Work

There exist similar approaches to employ compression or sparsity in DNNs, optimizing for different metrics.

ReSprop [3] uses pruning, quantization, and compression of activation maps during inference to accelerate the model and increase their representational power. This is crucial in real-time tasks and mobile deployment. However, this requires a pre-trained model of course.

Dithered Backprop [17] similarly uses a pruning and compression scheme, but on preactivation gradients to induce sparsity and additionally quantize non-zero values to low bit widths. Again, the goal is to achieve a speedup of the backward pass and to reduce computations, not memory. Additionally, the sparsity induced by Dithered Backprop is unstructured, which is only compatible with GPUs at extreme levels of sparsity.

Another very similar approach is presented in SWAT [12]. SWAT prunes activations during training based on magnitude after a dense forward computation with the goal of reducing FLOPs on sparse accelerators and thereby accelerate the training. During forward propagation SWAT additionally masks weights to that end. As with Dithered Backprop, the theoretical savings do not translate well to execution on a GPU.

In a previous work [1], partly based on SWAT, we used structured pruning of activations with the explicit goal of reducing the memory footprint during training. Although the encoding overhead shrinks with increasing block size of the sparse structure, there is a non-negligible overhead decoding the sparse structure in terms of computation and especially memory movements. The regularity of the pooling operation presented here eliminates the decoding overhead entirely.

## 3 Model Characterization

In this section we characterize the training memory footprint for various vision architectures and analyze properties of the activation tensors saved. We use a

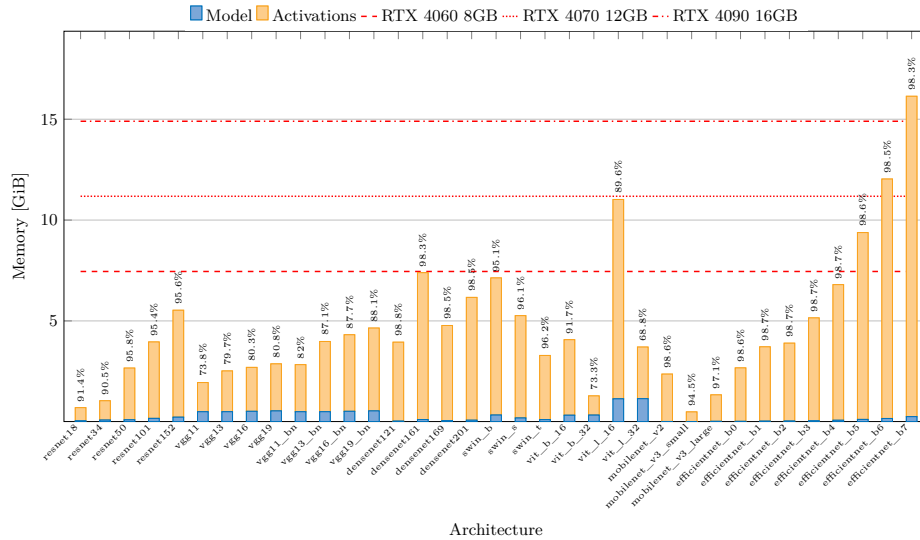


**Fig. 1.** Memory footprint during training of common vision architectures split into model parameters and activations. The ratio is heavily skewed toward activations. The most balanced is `vit_1_32` at 68.8% activations. On average, activations are responsible for 91.8% of the memory consumed. `EfficientNet_[B1-B4]` are the most extreme examples at 98.7% activations. The mini-batch size is 32 for all models. The red lines show the memory capacity of consumer-grade GPUs of the NVIDIA 4000 series for comparison. Note that the memory capacity is given in GB, while our measurements are in GiB. The printed percentages represent the proportion of activations in regard to the peak memory usage.

custom memory allocator to trace allocations in the `torchvision`<sup>3</sup> implementations of said architectures for detailed analysis. For peak values it is also possible to query PyTorch’s default allocator<sup>4</sup>.

As mentioned in Section 1, stored activations are responsible for most of the total memory consumed during training. Figure 1 compares the activation state to the model parameter state for various prominent vision architectures. Activations, on average, are responsible for 91.8% of the total memory consumed. The `EfficientNet`[15] architecture shows the most extreme split. Due to weight sharing, convolutional layers typically show a more skewed ratio than e.g. fully connected layers. On top of that, `EfficientNet` makes heavy use of point-wise and depth-wise convolutions in succession. This leads to 98.7% of the memory being consumed by activations in the case of `EfficientNet_[B1-B4]`. In contrast, `Vision Transformers` (ViT)[2] contain mainly fully-connected components, and therefore show less skew. Although, at 68.8% for `vit_1_32` activations still make

<sup>3</sup> <https://pytorch.org/vision/stable/index.html>

<sup>4</sup> [https://pytorch.org/docs/stable/generated/torch.cuda.max\\_memory\\_allocated.html](https://pytorch.org/docs/stable/generated/torch.cuda.max_memory_allocated.html)

up more than two thirds of the memory footprint. The activation footprint is also directly proportional to the mini-batch size. 32 is a fairly low value for most of the architectures listed. So the ratios shown here can be seen as best case values. Increasing mini-batch size skews the ratio further toward activations.

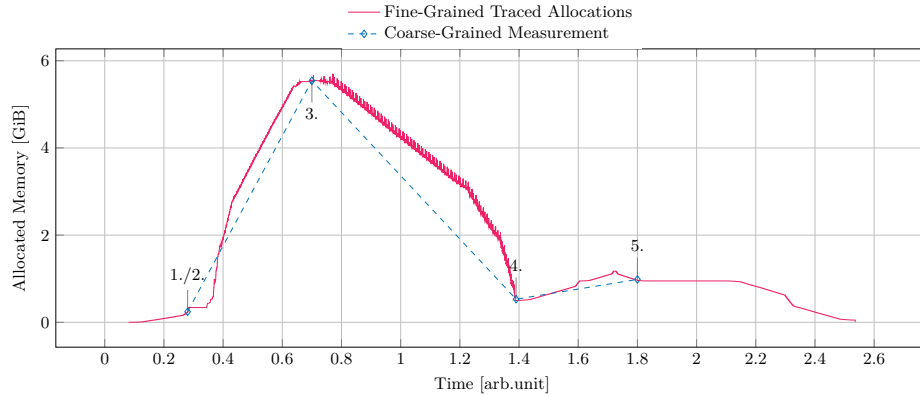


**Fig. 2.** Fine-grained tracing of allocations during model initialization and processing of a single mini batch of data for the **ResNet152** architecture. The red line shows the step-wise allocation of forward activations and the reverse as the backward computation unfolds. After the backward computation is completed, a second peak can be observed during the optimization stage. We can simplify this representation by only measuring at points of interest: model/input (1./2.) initialization, forward peak (3.), after backward (4.), optimizer peak (5.) represented by the blue marks.

The previous analysis only shows the peak memory consumption after the forward computation. However, allocation and deallocation of activations and other data is dynamic. Additionally, during the following optimization stage there may be additional memory allocations depending on the optimizer. A more detailed analysis is therefore needed to assess the potential for reduction of the memory footprint. Figure 2 shows the traced cumulated memory allocations at the example of the **ResNet152** architecture at mini-batch size 32. Based on the shape of the curve we can identify 5 points of interest that can be observed instead of tracing all allocations.

1. Model initialization: PyTorch allocates and initializes buffers for the model parameters (weights and biases).
2. Input data initialization: Allocate a tensor for an input mini-batch.
3. Forward pass peak: After the forward pass is completed memory usage is highest, as all activations have to be kept up to this point.
4. Backward pass complete: During backpropagation saved activations are successively deallocated, leading to a minimum once all gradients are calculated.

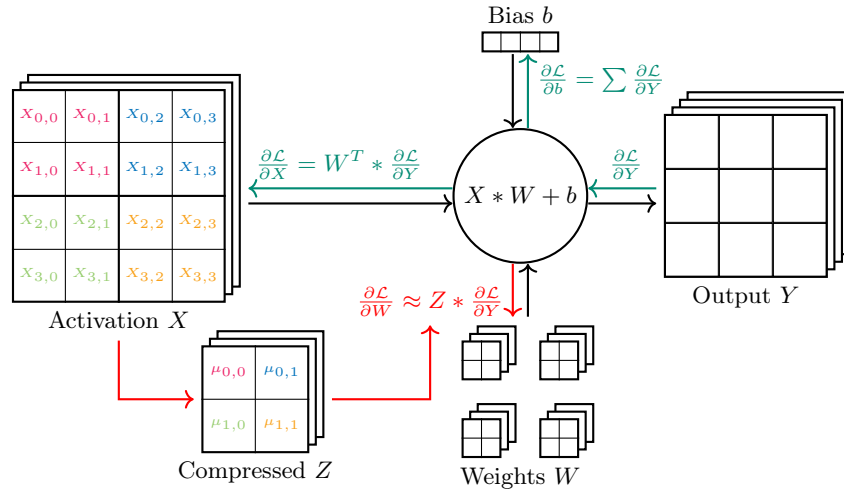


**Fig. 3.** Example of activation map compression for a convolutional layer. During the forward computation the input activation  $X$  is convolved with the weight tensor  $W$  and a bias  $b$  is added to produce output  $Y$ . Before saving the activation map for the backward pass, we compress it using pooling. Except for the original dimensions, this requires no additional encoding overhead. During backpropagation we inflate the compressed activation  $Z$  back to the original dimensions and use it to obtain the weight gradient, as shown in red. The other gradients, shown in green, are not affected by this, as they do not depend on the activations. This ensures that the propagated activation gradient remains accurate throughout the network. Only the weight updates themselves are imprecise.

5. Optimizer peak: During the optimization pass additional memory is required for momenta for example. This highly depends on the optimizer used. In this example, Adam.

## 4 Compressing Activation Maps

To address the problems related to encoding overhead for sparse data structures [14], we pursue a slightly different approach. Instead of encoding non-zero values we use average pooling to reduce the size of the activation maps. This has the substantial advantage that besides the pooling kernel size no additional encoding is needed, allowing us to drastically reduce the memory requirements.

Figure 3 shows the approach in detail. Forward-propagated activations are not compressed. We only apply pooling to input  $X$  after the output  $Y$  of the current layer is computed, yielding a compressed activation  $Z$ . By doing so, we always obtain an accurate loss value. The pooled activation  $Z$  is stored until it is used to calculate the weight gradient during backpropagation. With the kernel size of the pooling kernel we can now inflate the activation back to its original

dimensions and calculate the weight gradient normally. We are currently working on a custom implicit convolution kernel to elide the inflation and reduce memory transactions in addition to memory capacity.

In Figure 3 one can also observe how the computation of downstream gradients is changed based on the approximation of  $X$  by  $Z$ , e.g. by averaging. As denoted by the green color, both the downstream gradients  $\frac{\partial \mathcal{L}}{\partial X}$  and bias gradients  $\frac{\partial \mathcal{L}}{\partial b}$  are not affected by the compression. Thus, the propagated downstream gradient remains accurate and therefore does not accumulate errors through backpropagation. Only the weight updates  $\frac{\partial \mathcal{L}}{\partial W}$  become less accurate.

While in principle various forms of pooling are feasible, in this initial work we start with average pooling. Similarly, for more diversity in weight updates, one might change the pooling layout adaptively during training. Last, activation pooling could also be selectively disabled on a per-layer basis.

## 5 Experiments

We test the effects of our compression approach in terms of memory consumption and accuracy on **ResNet18**. We use the operator described in Section 4 to compress all activation maps throughout the network evenly. The stem convolution **conv1** as well as linear classifiers and batch normalization layers are kept unchanged. Figure 4 shows an overview of the architecture. We train on the ImageNet dataset using SGD and a step learning rate scheduler. The rest of the hyperparameters is kept close to the literature, except the mini-batch size, which we set to 64.

### 5.1 Training dynamics

Figure 5 shows the effects of compression on the training loss of ResNet. Compressing activation maps does not alter the trend of the loss curve, but only introduces an offset. This leads us to believe a longer training schedule might help to recover some of the accuracy lost by the compression. After 90 Epochs accuracies of 67.7%, 64%, and 50.1% are achieved at the mentioned levels of compression shown.

### 5.2 Layer sensitivity

To gain insight into the effects on an individual layer basis we compare the cosine similarity of the weight gradients after one epoch to a model trained without compression. Cosine similarity is formally defined as follows:

$$\cos(\mathbf{a}, \mathbf{b}) = \frac{\mathbf{a} \cdot \mathbf{b}}{\|\mathbf{a}\| \|\mathbf{b}\|} \quad (1)$$

A similarity of one means that gradients point in the same direction exactly, while one of minus one means the opposite. Thus, here a higher value is better.

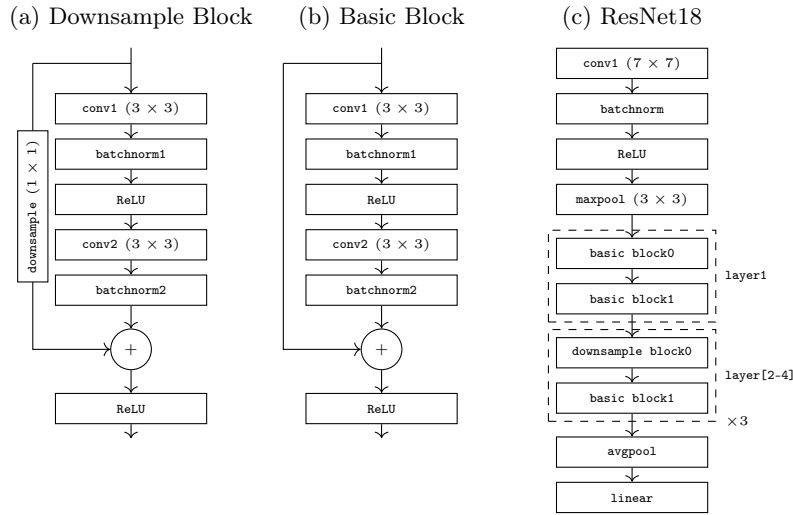


**Fig. 4.** Overview of the ResNet architecture (c) and its residual building blocks. The downsample block (a) features a  $(1 \times 1)$  convolution in the residual path, whereas the basic block (b) adds the input unaltered.

For this experiment we have fixed the data loader, so samples are processed by all models in the same order. Due to the stochastic nature of the optimizer, parameters diverge after the first epoch rendering a comparison meaningless. Figure 6 shows the similarities for **ResNet18** for brevity. However, the other variants show very similar trends. First, observing the uncompressed stem convolution **conv1** shows that the gradient is indeed unaffected, as shown in Figure 3. Next, we can see that the effects are not uniform across layers. In the first sublayer **conv1** deviates further from the baseline, while in the second sublayer it is **conv2**. This may be a result of the gradient flow around the skip connections. Downsample layers seem to be more resilient to compression. This is most likely due to the reduced kernel size of  $(1 \times 1)$ .

### 5.3 Memory footprint reduction

Because compression does not introduce significant encoding overhead, we are able to drastically lower the memory consumed by activations. Table 1 shows the memory consumed by both weights and activations for all convolutional layers in ResNet18. Additionally, the table also shows the consumption for  $(2 \times 2)$  and  $(4 \times 4)$  compressed activations. As expected, pooling reduces the memory requirement by  $\frac{3}{4}$  and  $\frac{15}{16}$  respectively, which amounts to roughly 191 MiB and 239 MiB.

With regard to the total memory footprint, the other layers have to be taken into account as well. At around 670 MiB total activation state,  $(2 \times 2)$  compression

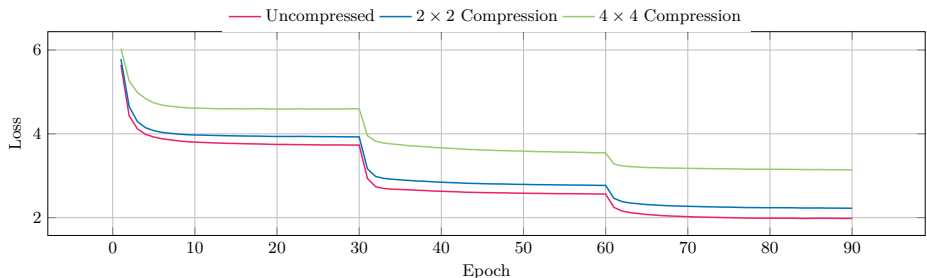


**Fig. 5.** Training loss for **ResNet18** trained on ImageNet using SGD with momentum and step learning rate scheduler. Compression seems to introduce an offset to the loss curve.

of the convolutional layer’s activations results in a 29% reduction and  $(4 \times 4)$  in a 36% reduction of the overall memory footprint.

#### 5.4 Maintaining accuracy

To restore some of the lost accuracy due to compression, experiments with more training epochs were conducted. The goal is to find a viable trade-off between the increased end-to-end training time and the reduced memory consumption. Extending the training schedule from 90 to 120 epochs indeed shows improvements, especially in the case of  $(2 \times 2)$  compression. We are able to come within 1.3% of the baseline accuracy, which we view as acceptable, considering the fluctuations based on weight initialization being only slightly smaller.  $(4 \times 4)$  compression results are still unacceptable.

## 6 Discussion and Future Work

This work is still in progress, but the preliminary results seem promising and we intend to expand the concept further. Next steps include more architectures, especially EfficientNet on the CNN side and Transformers like ViT and swin. For EfficientNet in particular we expect good results, based on the observations made on the  $(1 \times 1)$  downsample convolutions. Additionally, we plan on expanding compression to batch normalization layers as well, as they produce activations with the same dimensions of the respective convolutional layer. Non-uniform pooling kernel shapes could also be considered.

The results from Figure 5 show that a uniform  $(4 \times 4)$  compression is not viable. However, with  $(2 \times 2)$  compression alone, we are able to reduce the peak memory usage by 29%. Considering Figure 1, a reduction by 29% would, in many cases, allow for the use of a "smaller" GPU, going from a 4090 to a 4080 for example in the case of **EfficientNet\_B7**. For tasks like fine-tuning and retraining even embedded devices like the Jetson Nano series become viable. With the custom compressed backward convolution in place, we plan on running

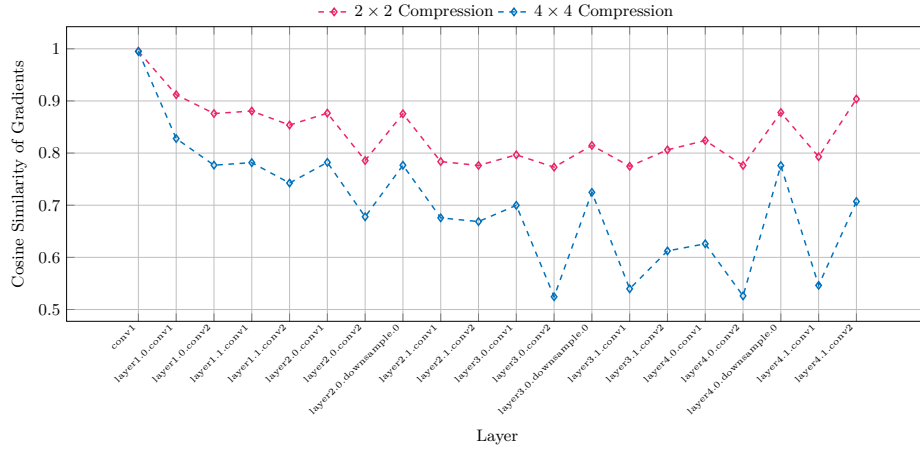


**Fig. 6.** Capturing the cosine similarity of the weight gradients of a **ResNet18** after one epoch compared to an uncompressed model shows that not all layers are affected equally by compression. Downsample layers seem to be the least affected, while **conv2** seems to be especially sensitive in sublayer zero and **conv1** in sublayer one.

**Table 1.** Memory consumption per convolutional layer with respect to parameters  $W$ , activations  $X$ , and compressed versions  $Z$ . To keep consistent with Figure 1 a mini-batch size of 32 is assumed here.

Layer	$W$ [MiB]	$X$ [MiB]	$Z$ (2 × 2) [MiB]	$Z$ (4 × 4) [MiB]
conv1	0.04	18.38	4.59	1.15
layer1.0.conv1	0.14	24.50	6.12	1.53
layer1.0.conv2	0.14	24.50	6.12	1.53
layer1.1.conv1	0.14	24.50	6.12	1.53
layer1.1.conv2	0.14	24.50	6.12	1.53
layer2.0.conv1	0.28	24.50	6.12	1.53
layer2.0.conv2	0.56	12.25	3.06	0.77
layer2.0.downsample.0	0.56	24.50	6.12	1.53
layer2.1.conv1	0.56	12.25	3.06	0.77
layer2.1.conv2	1.12	12.25	3.06	0.77
layer3.0.conv1	2.25	12.25	3.06	0.77
layer3.0.conv2	2.25	6.12	1.53	0.28
layer3.0.downsample.0	2.25	12.25	3.06	0.77
layer3.1.conv1	4.50	6.12	1.53	0.28
layer3.1.conv2	9.00	6.12	1.53	0.28
layer4.0.conv1	9.00	6.12	1.53	0.28
layer4.0.conv2	9.00	3.06	0.56	0.06
Sum	41.94	254.19	63.34 (-75%)	15.35 (-94%)

experiments on a Jetson Orin Nano device including tasks like retraining and online learning in the future.

As yet, the process is also fairly invasive. Custom implementations of the network architectures are required. We therefore plan to integrate the compression operators in to our structured sparse operator library `deep-sparse-nine` for a more streamlined workflow. This would also allow to easily mix compression and sparsity.

Regarding the methodology, cosine similarity data could be used to automatically find a viable per-layer configuration, perhaps even adaptively during training via control epochs. At the cost of additional training time, one could initialize an uncompressed model to repeat the cosine similarity analysis shown in subsection 5.2 mid-training. Based on the data, individual layers could be updated to a new kernel size or trained uncompressed for a period of time.

Our Code is available on GitHub: [https://github.com/danielbarley/cnn\\_mean\\_compression](https://github.com/danielbarley/cnn_mean_compression).

**Acknowledgments.** This work is part of the "Model-Based AI" project, which is funded by the Carl Zeiss Foundation.

**Disclosure of Interests.** The authors have no competing interests to declare that are relevant to the content of this article.

## References

1. Barley, D., Fröning, H.: Compressing the backward pass of large-scale neural architectures by structured activation pruning. 6th Workshop on Accelerated Machine Learning (AccML), collocated with HiPEAC 2024 Conference (2023), <https://arxiv.org/abs/2311.16883>
2. Dosovitskiy, A., Beyer, L., Kolesnikov, A., Weissenborn, D., Zhai, X., Unterthiner, T., Dehghani, M., Minderer, M., Heigold, G., Gelly, S., Uszkoreit, J., Houlsby, N.: An image is worth 16x16 words: Transformers for image recognition at scale. In: International Conference on Learning Representations. ICLR (2021), <https://openreview.net/forum?id=YicbFdNTTy>
3. Goli, N., Aamodt, T.M.: Resprop: Reuse sparsified backpropagation. In: IEEE/CVF Conference on Computer Vision and Pattern Recognition. CVPR (2020). <https://doi.org/10.1109/CVPR42600.2020.00162>
4. He, K., Zhang, X., Ren, S., Sun, J.: Deep residual learning for image recognition. In: IEEE Conference on Computer Vision and Pattern Recognition. CVPR (2016). <https://doi.org/10.1109/CVPR.2016.90>
5. He, Y., Zhang, X., Sun, J.: Channel pruning for accelerating very deep neural networks. In: IEEE International Conference on Computer Vision. ICCV (2017). <https://doi.org/10.1109/ICCV.2017.155>
6. Howard, A.G., Zhu, M., Chen, B., Kalenichenko, D., Wang, W., Weyand, T., Andreetto, M., Adam, H.: Mobilenets: Efficient convolutional neural networks for mobile vision applications. CoRR **abs/1704.04861** (2017), <http://arxiv.org/abs/1704.04861>

7. Jacob, B., Kligys, S., Chen, B., Zhu, M., Tang, M., Howard, A., Adam, H., Kalenichenko, D.: Quantization and training of neural networks for efficient integer-arithmetic-only inference. In: IEEE/CVF Conference on Computer Vision and Pattern Recognition. CVPR (2018). <https://doi.org/10.1109/CVPR.2018.00286>
8. Krieger, T., Klein, B., Fröning, H.: Towards Hardware-Specific Automatic Compression of Neural Networks. 2nd International Workshop on Practical Deep Learning in the Wild, collocated with 2023 AAAI Conference on Artificial Intelligence (2022), <https://arxiv.org/abs/2212.07818>
9. Micikevicius, P., Narang, S., Alben, J., Diamos, G., Elsen, E., Garcia, D., Ginsburg, B., Houston, M., Kuchaiev, O., Venkatesh, G., Wu, H.: Mixed precision training. In: International Conference on Learning Representations. ICLR (2018), <https://openreview.net/forum?id=r1gs9JgRZ>
10. Prechelt, L.: Connection pruning with static and adaptive pruning schedules. *Neurocomputing* **16**(1), 49–61 (1997). [https://doi.org/https://doi.org/10.1016/S0925-2312\(96\)00054-9](https://doi.org/https://doi.org/10.1016/S0925-2312(96)00054-9)
11. Qin, H., Gong, R., Liu, X., Bai, X., Song, J., Sebe, N.: Binary neural networks: A survey. *Pattern Recognition* **105**, 107281 (2020). <https://doi.org/https://doi.org/10.1016/j.patcog.2020.107281>
12. Raihan, M.A., Aamodt, T.: Sparse weight activation training. In: Advances in Neural Information Processing Systems. NIPS (2020), [https://proceedings.neurips.cc/paper\\_files/paper/2020/file/b44182379bf9fae976e6ae5996e13cd8-Paper.pdf](https://proceedings.neurips.cc/paper_files/paper/2020/file/b44182379bf9fae976e6ae5996e13cd8-Paper.pdf)
13. Roth, W., Schindler, G., Klein, B., Peharz, R., Tschitschek, S., Fröning, H., Pernkopf, F., Ghahramani, Z.: Resource-efficient neural networks for embedded systems. *Journal of Machine Learning Research* **25**(50), 1–51 (2024), <http://jmlr.org/papers/v25/18-566.html>
14. Schindler, G., Roth, W., Pernkopf, F., Fröning, H.: Parameterized structured pruning for deep neural networks. In: Machine Learning, Optimization, and Data Science (2020). [https://doi.org/10.1007/978-3-030-64580-9\\_3](https://doi.org/10.1007/978-3-030-64580-9_3)
15. Tan, M., Le, Q.: EfficientNet: Rethinking model scaling for convolutional neural networks. In: 36th International Conference on Machine Learning (2019), <https://proceedings.mlr.press/v97/tan19a.html>
16. Tang, Z., Shi, S., Wang, W., Li, B., Chu, X.: Communication-efficient distributed deep learning: A comprehensive survey. *CoRR* **abs/2003.06307** (2023), <https://arxiv.org/abs/2003.06307>
17. Wiedemann, S., Mehari, T., Kepp, K., Samek, W.: Dithered backprop: A sparse and quantized backpropagation algorithm for more efficient deep neural network training. In: IEEE/CVF Conference on Computer Vision and Pattern Recognition Workshops. CVPRW (2020). <https://doi.org/10.1109/CVPRW50498.2020.00368>
18. Zhao, H., Liu, D., Li, H.: Efficient integer-arithmetic-only convolutional networks with bounded relu. In: IEEE International Symposium on Circuits and Systems. ISCAS (2021). <https://doi.org/10.1109/ISCAS51556.2021.9401448>